

DESIGN AND CONTROL OF A FORCE-REFLECTING HAPTIC INTERFACE FOR TELEOPERATIONAL GRASPING

Scott L. Springer

University of Wisconsin – Stout, Department of Technology
332 Fryklund Hall
Menomonie, WI 54751
springers@uwstout.edu

and

Nicola J. Ferrier

University of Wisconsin – Madison, Department of Mechanical Engineering
1513 University Avenue
Madison, Wisconsin 53706
ferrier@engr.wisc.edu

Abstract

In this paper the design of a multi-finger force-reflecting haptic interface device for teleoperational grasping is introduced. The haptic interface or “master” controller device is worn on the human operator’s hand and measured human finger positions are used to control the finger positions of a remote grasping manipulator or “slave” device. The slave may be a physical robotic grasping manipulator, or a computer-generated representation of a human hand such as used in virtual reality applications. The forces measured by the robotic slave, or calculated for the virtual slave, are presented to the operator’s fingertips through the master providing a means for improved human sensation of presence and better control of grasping tasks in the slave environments. Design parameters and performance measures for haptic interfaces for teleoperation are discussed. One key performance issue involves the high-speed display of forces during initial contact, especially when interacting with rigid surfaces. The present design reduces slave controller computational requirements and overcomes actuator response time constraints thus addressing the problematic issue of the display of rigid bodies.

The design presented utilizes a planar four-bar linkage for each finger, to represent each finger bend motion as a single degree of freedom, and to provide a finger bend resistance force that is substantially perpendicular to the distal finger pad throughout the full 180 degrees of finger bend motion represented. The finger linkage design, in combination with a remote position measurement and force display assembly, provides a very light weight and low inertia system with a large workspace. The concept of a replicated finger is introduced which, in combination with a decoupled actuator and feed forward control, provides improved performance

in transparent free motion, and rapid, stable touch sensation of initial contact with rigid surfaces. A distributed computation architecture with a PC based haptic interface controller and associated control algorithms are also discussed.

1. Introduction

A haptic interface, often called a “master,” is used to measure the positions of an operator’s body, and utilize these positions to control the motion of a remote manipulator or “slave”. A haptic display provides haptic feedback. Thus a haptic interface and display presents to the operator, through the master, a touch sensation representing the touch sensations experienced by the slave (Burdea, 1996). In this paper, a new design of a haptic interface with display is discussed. Our design is for an interface capable measuring several fingers’ motion, and displaying force to several fingers. In teleoperation, the slave hand or manipulator may be either a robotic hand capable of grasping motions, or a “virtual” hand, often utilized in virtual reality simulations. A virtual hand merely consists of a computer-generated image of a hand that is used to interact with a computer-simulated environment. Applications of teleoperation may therefore be divided into those of a virtual reality type or those of a physical type. Popular virtual reality applications include computer-aided design, training, and entertainment, while physical teleoperation applications include space missions, underwater exploration and manipulation in toxic environments. The value of haptic display as an interface for teleoperational grasping is that the operators can use their highly developed natural motor skills to very precisely control the slave manipulator (Shimoga, et.al., 1996). In virtual reality applications, the value is that the operator experiences a more realistic sense of immersion in the virtual environment, and the “virtual” environment more closely resembles “reality”.

2. Background

While many haptic interfaces have been proposed, a common feature lacking in prior designs is the ability to accurately represent rigid bodies. Traditional design of force reflecting haptic interfaces employs one or more actuators such as motors or fluid piston-cylinders directly coupled to the human operator during use (Burdea, 1996). Thus when the operator executes a motion, in the absence of contact between the slave and any object in the slave environment, the operator back drives the actuator, and when the slave contacts an object in the slave environment, the actuator is powered to provide a force sensation to the operator. In virtual environments, the force is typically calculated as a function of the slave penetration distance (x) into the object, the slave's velocity (x'), and the virtual object's properties. The force is often calculated by:

$$F = Kx + Bx' \quad (1)$$

where K is the stiffness of the object and B is the damping coefficient of the object. In physical teleoperation, the force to be displayed by the master is typically measured at the slave by a force sensor. One problem area that has been repeatedly cited in the virtual applications literature is that the master of a traditional design is not capable of display of very rigid or hard objects. When the values of K and B in EQ. 1 are set to very high values, undesirable oscillations often occur, and the touch sensation experienced by the operator is quite unnatural (Burdea, 1996), (Colgate, et.al. 1993), (Kazerooni, 1993). In teleoperation, the time lag between force sensing at the slave and force display by the master requires that all master motions be limited in velocity. For example in a physical teleoperational experiment by Shimoga, et.al. (1996), a three finger grasp required 20 seconds, whereas a real human hand grasp is completed in as little as 100 milliseconds (Klatzky, et. al., 1996). If artificial master velocity limits are not included as part of the system, very high forces of contact between the slave and grasp object are likely to occur, resulting in damage to the robot or the grasped object. For human grasping, initial contact forces can be highly transient in nature. Sculteis et.al.(1996) shows force transients with a slope of $1.5 \text{ N} / 0.1 \text{ s}$ in a tele-operation task, while Lawrence et.al. (1996) show force transients of up to $2 \text{ N} / 0.005 \text{ s}$ during a tap on a virtual wall, and thus delay in the haptic display can cause excessive force to be applied by the manipulator fingers. The haptic interface design and control algorithm discussed in this paper addresses both representation problems of virtual rigid bodies in a stable (non-oscillatory) manner and rapid response force display for more natural grasping in physical teleoperation. Springer and Ferrier (1999) give a detailed analysis of the dynamics involved during initial contact for both traditional interface design and the new design discussed in this paper.

It has been recognized that a single degree of freedom (DOF) can be used to represent (approximately) the finger tip position with respect to the palm. A single DOF angular representation is shown in FIG. 1. Although the exact position of the distal fingertip pad is not constrained to follow this path, it has been observed that typical human finger motion does in fact follow a repeatable path as indicated in the figure. This observation has been used in virtual reality finger measuring devices and algorithms, wherein the angle

of finger bend is measured at the operator's hand and utilized to control the virtual finger's position as a single control variable (e.g. Cyberglove, Virtual Technologies, 1997). Another observation by Springer and Gadh, (1997) is that during contact with objects to be grasped the primary forces commonly experienced by the finger are those directed normal to the surface of the fingertip distal pad. Forces in this direction are deemed the most useful for a variety of virtual reality computer aided design tasks, as well as precision teleoperational grasping tasks.

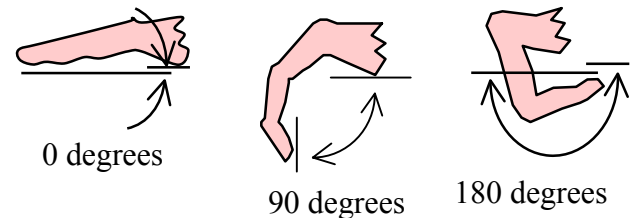


Figure 1 – Representation of Finger Motion by a Single Variable

Previous attempts at hand mounted single controlled degree of freedom finger tip force displays have provided forces that vary widely with finger bend angle, and/or are able to represent motion through only a fraction of the 180 degrees of real finger bend motion. For example, the palm mounted air cylinder method of Burdea's (1996) RMI and RMII provide a force at an angle that widely varies with finger bend angle, and can only represent finger bend from approximately 40 to 90 degrees. The angle of applied force also varies with finger bend angle for the tendon approach of Kramer (1993). The tendon with additional moment arm modification of Virtual Technologies (1997), more closely provides normal direction fingertip forces throughout full finger bend range, but at the expense of applying ghost forces to the back of the second finger phalange.

3. System Mechanical Design

The concept utilized for this design is based on the prioritization of the modalities and degrees of freedom within the haptic senses. The modalities and controlled degrees of freedom were prioritized with the most important being those capable of representing the widest range of dexterous manipulation tasks. From the prioritization study it was concluded that forces to multiple fingertips in the normal direction provided the most valuable haptic display for grasping operations (Springer and Gadh, 1996, 1997). This type of display is consistent with "precision grasp of highest dexterity" as found by Cutkosky and Howe (1990). To implement this mode of display, it was first recognized that in order to display forces to multiple fingertips, development of a portable haptic display wherein the mechanism reaction forces were grounded to the operator's body in a location near the fingertips, offered significant advantages. These advantages include low mass of the mechanical structure carried by the operator in changing hand positions, lack of hand workspace limitations, and the ability to develop a simple, lightweight structure for contact force display. The disadvantage of this approach is that global force to the hand as described above can not be truly represented unless the haptic interface is attached to a master robot.

In this application, it may be desirable to not have the haptic interface contain an earth grounding linkage, so that the hand position and orientation measurement can be attached to a master robot arm of the same design as the slave robot arm. For VR applications, position and orientation measurement of the hand as a single point is readily available in the form of a magnetic tracker, such as Flock of Birds (Ascension, 1998).

The present interface utilizes a four link serial planar mechanism for transmitting force resistance to finger bend toward the palm. The same linkage is utilized for transmitting output motion of the finger bend (or position of the fingertip with respect to the back of the hand) to a linear motion of a flexible sheathed cable. The hand mechanism for a single finger is shown in FIG. 2, and is provided with three rotational degrees of freedom, matching those of the finger in its longitudinal plane. The mechanism is also configured such that position measurement and/or force input to one of the three degrees of freedom is sufficient to represent the natural finger bend motion or restriction thereof.

The mechanism of the mounted interface in combination with the human hand forms a six bar closed loop kinematic chain as shown in FIG 2.

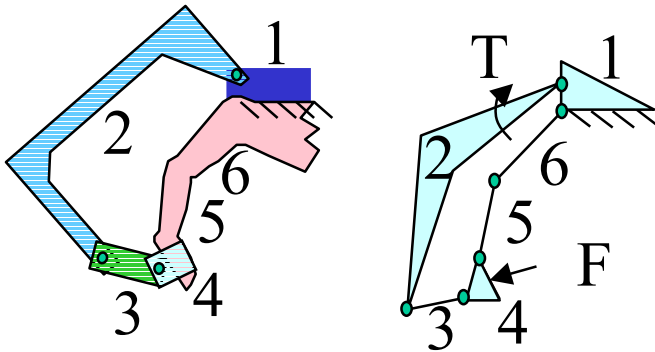


Figure 2 - Six Bar Linkage Formed When Operator Wears Haptic Mechanism

The six bar chain consists of the hand outer surface and the hand attachment of the hand mechanism, which together make up link 1, which is the ground link. Connected to the ground link is link 2, the inverted “U” shaped link of the interface hand mechanism, which is in turn pivotally connected to link 3. Link 3 is pivotally connected to link 4, which comprises the fingertip thimble and the finger distal phalange. Link 5 forms a pivotal connection with link 4 and link 6, comprising the second finger phalange, while link 6 comprises the proximal finger phalange.

In this linkage design, the driver for clockwise rotation is link 2, driven to simulate interference with an object. However, links 4, 5, 6 can also drive the linkage for both clockwise and counter-clockwise rotation. As can be seen from FIG 3, the six bar chain permits an approximate perpendicular angle formation between link 4 and link 3 throughout the range of motion. Because link 3 is a two force member, the force between links 3 and 4 is directed along a line formed by the two revolute joints of link 3. Considering this line of action for the force presented to the operator, one can

evaluate the directional error of the force applied, with respect to normal to the distal phalange (link 4).

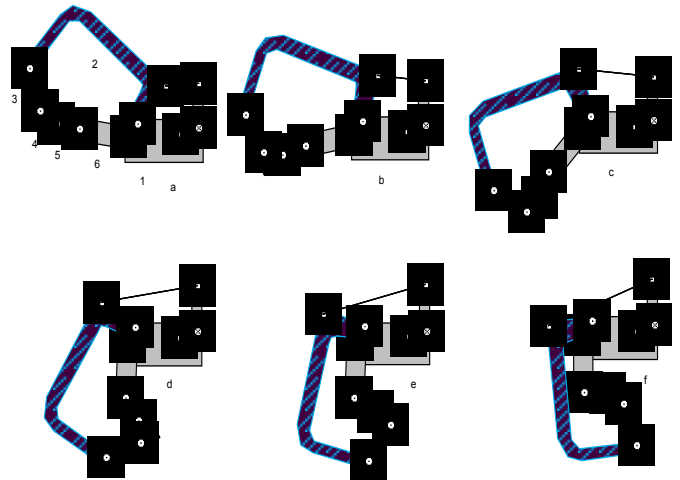


Figure 3 Positions of Six Bar Chain During Grasp

For the positions shown, the errors are as follows: (a) -20° , (b) 0° , (c) $+17^\circ$, (d) $+19^\circ$, (e) $+30^\circ$, and (f) -18° . It may appear initially that an error as large as 30° would be problematic, but a closer inspection such as given in FIG. 4, demonstrates human adaptation to the application of the highest directional error of FIG. 3e. FIG. 4 shows an observed positional adjustment by the operator during a force application, to compensate for an initial force application angle of 30° off perpendicular.

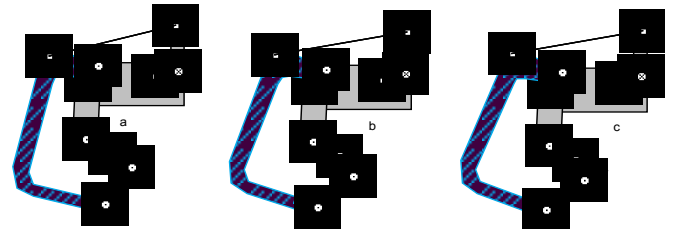


Figure 4 - Rotation of Distal Phalange During Force Application

It appears from preliminary experimentation that in this type of compensation the operator can choose not to compensate for directional error, or, in the absence of a concentrated effort, will automatically compensate for the error. This results in a change of finger joint angles from FIG. 4a to that of FIG. 4c, wherein the applied force assumes a normal direction. For situations when the operator does not compensate for off-normal directions, the haptic sensation (for angular errors less than 30°) does not appear erroneous. This is presumably due to the ability to sense relatively large magnitude forces primarily in the normal direction. Thus, a benefit of the linkage design is that throughout 180 degrees of motion for the finger, resistance forces are applied approximately normal (within 30°) to the distal finger pad, accurately representing

the direction of normal forces that occur during real grasping and manipulation of objects.

The hand-mounted mechanism is capable of representing the fingertip position, throughout a wide range of grasping motions (FIG. 3). The motion of the finger during grasp can be represented as a single variable, indicated by the rotational position of link 2. This single variable representation is not unique because several relative link angles are possible. The range of relative link angles is quite small and thus introduces a small amount of uncertainty in fingertip position. A benefit is that because there are two uncontrolled degrees of freedom, the linkage is effective for a variety of operator's hand sizes, without the need for adjusting link lengths.

The rotational motion of link 2 is transmitted via a sheathed cable to a remotely mounted pivotal link, and called a replicated finger. This approach permits position measurement and force application apparatus to be remotely located, and the operator need not carry the bulk and weight of these systems. The replicated finger (as shown in FIG. 5) pivots on the input shaft of the position measurement potentiometer that converts the motion of the replicated finger into an analog voltage signal. The voltage signal is thus proportional to the degree of finger bend. This signal is read into the haptic control PC by a data acquisition (DAQ) board. The analog voltage signal is converted to a digital value for use in controlling the slave finger positions and in various control calculations as described in the following sections 4.

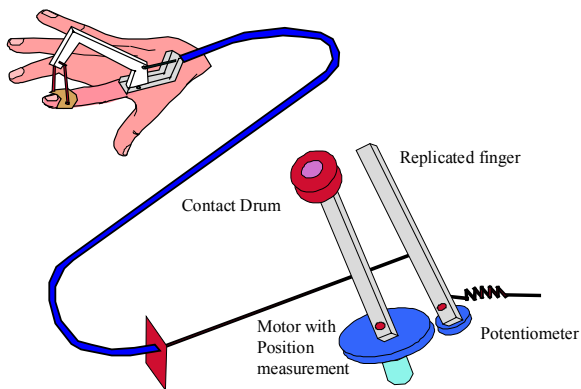


Figure 5 - Hand Mounted Mechanism, Measurement & Force Display

The replicated finger described above is also used to present forces to the fingertip that resist finger inward bend. This is possible because the replicated finger accurately reflects the motion of the operator's finger as a single degree of freedom pivoting link, and resistance to motion of the replicated finger provides a proportional resistance to the operator's finger. The contact drum provides the resistance to replicated finger motion. The drum occupies a position that under control of the computer selectively interferes with replicated finger rotation. After initial contact the force available at the contact drum is controlled by pulse width modulation (PWM) through the haptic control PC.

Thus, the mechanical system described above is capable of transmitting finger position, selectively defining interfering and non-interfering positions, and displaying a variable and controllable force magnitude. This is done while requiring only minimal control I/O of replicated finger position measurement, motor position measurement, and digital motor output. The number of control parameters is very important, because the cost and computer execution time both increase with the number of control parameters. Further details on the design of the system are given by Springer (1999).

4. System Control Algorithm

Given the single variable representation of finger motion, we can map the finger bend angle to a position of the "replicated finger". The contact drum can be controlled to track the replicated finger position, offset by a few degrees. The contact drum can be controlled to maintain a constant position preventing replicated finger counter-clockwise rotation and thus preventing finger retraction. Alternatively, the contact drum can be controlled to provide a variable magnitude force to the replicated finger that is transferred to the operator's finger. A detailed description of this control algorithm we call DECAFF (DE-Coupled Actuator with Feed Forward control) is described in this section.

The control system includes a distributed computing platform as has been utilized extensively in the haptics field. The present platform consists of a low end PC for execution of all haptic device data acquisition and control algorithms, connected by a serial line to either a slave manipulator control computer, or a virtual reality simulation computer. The haptic control PC software is implemented in C++ language. The C++ code is capable of an execution cycle less than 1 ms (1000 Hz) for all five fingers. The haptic control code has three main algorithms: (1) configure multi-function I/O board and calibrate for the individual user finger motion, (2) contact position control for initial contact with virtual objects, (3) variable magnitude force display control. The configuration and calibration algorithm performs DAQ board initialization functions and a user calibration routine. The calibration routine requests the operator to fully extend and retract their fingers, during which the program records the minimum and maximum voltage signal delivered by the finger bend potentiometers. Subsequently, the finger bend angle (β) is then calculated by:

$$\beta[i] = 180 * (\text{read_volt}[i] - \text{pos_low}[i]) / (\text{pos_high}[i] - \text{pos_low}[i]) \quad (2)$$

where:

β_i = the current position of finger i (in degrees)

$\text{read_volt}[i]$ is the current voltage of replicated finger potentiometer for finger i

$\text{pos_low}[i]$ is the lowest voltage value recorded for finger i during calibration finger extension and retraction (which corresponds to the fully extended finger at a 0 degree position)

pos_high[i] is the highest voltage recorded for finger i during calibration finger extension and retraction (which corresponds to a fully retracted finger in the 180 degree position)

This delivers a value of 0 to 180 degrees for the current position of finger (i), wherein 0 degrees corresponds to a fully extended finger and 180 degrees reflects a finger position completely retracted to the palm (FIG. 1). In order to calibrate the motor position control, a screen prompt asks the user to fully retract their fingers and allow the contact drum to extend the fingers under a loose grasp. The control algorithm then advances the contact drum, periodically recording the voltage of the motor position potentiometer when the finger bend is at predetermined intervals. This mapping yields a contact drum position accuracy of +/- 2 degrees with respect to the replicated finger position for recorded replicated finger position intervals of 20 degrees.

For the present implementation test bed, the global position of the hand is not recorded, as only the grasp task is under investigation. However, it would be possible in other applications to attach the haptic display to a master robotic arm which, in turn, would control a duplicate slave robotic arm equipped with a grasping end effector similar to that of the of the implementation test bed. Alternatively, especially for VR applications, the global position and orientation of the hand in the virtual space can be provided by a commercial tracking device, shown as cube on back of hand in FIG. 6.

Position control variables for each finger denoted by subscript i are shown in FIG. 6. The interface between the master controller and the slave controller is shown in FIG. 7. Finger bend angle (β) is provided by periodic calls to the finger bend routine described above. Bend angle (β) is measured at the master and sent to the slave to control the position of the slave finger. Pre-contact distance (α) and force magnitude (F) are measured (or calculated) at the slave and sent to the master to control the contact drum position or force. The goal of providing fast response and highly stable contact sensation display is accomplished by selectively controlling the position or force of the contact drum as follows. Prior to contact between the slave and any slave environment object, the force (F) sent by the slave to the master is zero and the pre-contact distance (α) is greater than zero. In this case, position control is used. If there are no objects within the range of pre-contact distance (α) sensing, the value of α sent by the slave is a maximum range value (α_{max}). If an object is within the range of distance sensing, the measured or calculated value of α and a force (F) of zero is sent by the slave to the master for each finger. The master controller uses the received distance value (α_i) to calculate the contact drum position (γ_i) for each finger (i) as follows.

If pre-contact distance (α_i) is greater than a predetermined offset distance (α^*), the contact drum for finger (i) is controlled to assume a position (γ_i) as:

$$\gamma_i = \alpha_i + \beta_i \quad \text{for } (\alpha_i > \alpha^*) \quad (3)$$

If the operator moves a finger (i) closer toward the palm, so as to cause the slave finger (i) to become closer to an object in the slave

environment than the offset distance (α^*), the proximity contact drum position (γ_i^*) is defined as:

$$\gamma_i^* = \alpha_i + \beta_i \quad \text{for } (\alpha_i(t) \leq \alpha^*) \quad (4)$$

$$\text{and } (\alpha_i(t-1) > \alpha^*)$$

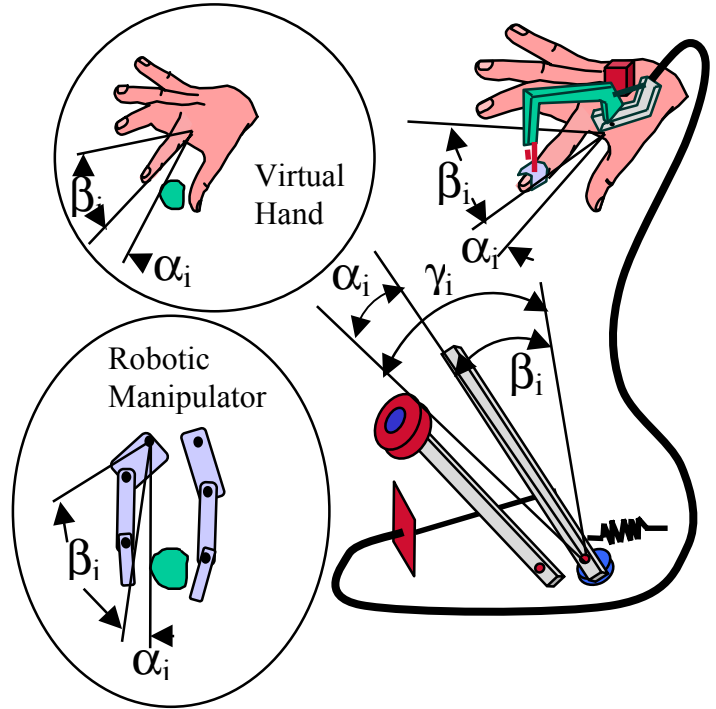


Figure 6 – Position Control Variables

Where $\alpha_i(t)$ is the pre-contact distance of the current calculation cycle and $\alpha_i(t-1)$ is the pre-contact distance of the previous calculation cycle. While the slave finger is closer to an object than the offset distance (α^*), the contact drum is controlled to maintain the proximity position (γ_i^*).

$$\gamma_i = \gamma_i^* \quad \text{for } (\alpha_i \leq \alpha^*) \quad (5)$$

For slave objects that are rigid or have a high stiffness (K) and/or high damping (B), the force (F_i) sent to the master by the slave makes a (nearly) instantaneous step from a value of 0 to 100%. In this case, position control is continued.

$$\gamma_i = \gamma_i^* \quad \text{for } (F_i \geq 100\%) \quad (6)$$

For slave objects of lower stiffness and damping, the force will more gradually increase with the penetration distance (x) and velocity (x'). With these objects the slave sends a contact force:

$$0 < F_i < 100 \quad (7)$$

In this case, the [haptic](#) master controller executes the variable magnitude force control algorithm.

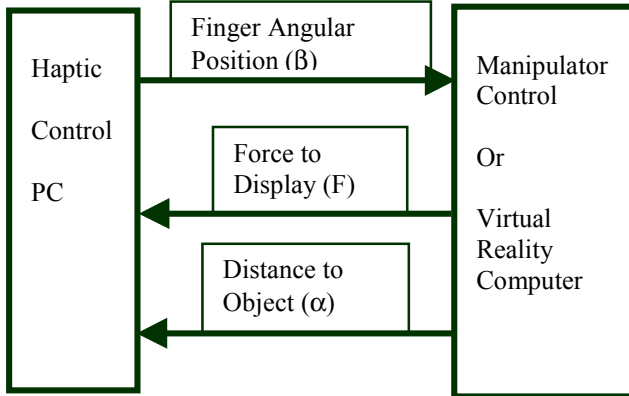


Figure 7 - Interface definition

To display a variable magnitude force, the control algorithm uses pulse width modulation (PWM) torque control to the motor driving the contact drum as shown in FIG.8. The force applied to the operator's fingertip is proportional to the motor torque.

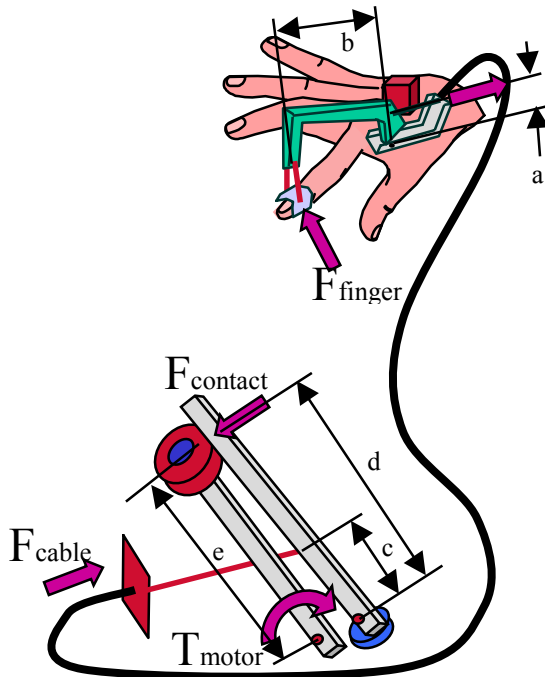


Figure 8 – Variable Force Display

Neglecting cable friction, the fingertip force is given by the following geometry based (constant) function of motor torque..

$$F_{\text{finger}} = (a/b) * (d/c) * (1/e) * T_{\text{motor}} \quad (8)$$

Where lengths a, b, c, d, and e are depicted in FIG. 8

Knowing the desired force to be displayed, either by a scale of manipulator force or determined as a function of penetration distance and object stiffness (EQ. 1), and by *a priori* measurement of the maximum fingertip force that can be delivered by the system, we can present a PWM ($\Phi = \% \text{ of stall torque}$) controlled force as follows.

$$\Phi = F_{\text{finger}}(\text{desired}) / F_{\text{finger}}(\text{max}) \quad (9)$$

The force delivered is dependent on the penetration distance, and as with prior haptic displays during this mode the penetration distance will be that given by the previous finger bend input and virtual reality environment calculation. To implement PWM force control within the haptic PC, several motor control calculation cycles are required. The basic implementation is such that for a given percentage of maximum force (Φ), the motor digital output is given an “on” signal for a corresponding percentage of calculation cycles followed by an “off” signal for $(1 - \Phi)$ cycles. For example an 80% of stall force ($\Phi = 0.80$) is delivered by giving 4 “on” signals to the motor followed by 1 “off” signal, repeating the sequence.

5. Human Perception Experiment

In order to evaluate the effectiveness of the mechanical and control system described above, a human perception experiment was conducted. This section provides a preliminary report of the results of these experiments, while more detailed data analysis is currently being prepared for publication (see Springer, 1999). Each subject was asked to compare the touch sensation experienced when in contact with a variety of surface pairs. One surface of each pair was controlled by the DECAFF method, while the other was controlled by a traditional haptic display control algorithm. Subjects were initially trained in how the system functioned, wearing a single finger mechanism as described above. For initial training, subjects could watch a virtual finger motion follow that of their real finger, and could feel the touch sensation as the virtual finger contacted a virtual surface. After the training session, subjects were not permitted to see the virtual finger monitor and thus had to rely solely on the touch sensation to report their perceptual experience. The experiment was designed as a two level, three variable factorial design, conducted with both a traditional control algorithm and with the proposed DECAFF system described herein. The traditional control system was implemented with the hardware described in this paper, modified to include a control algorithm to model a traditional design (described in section 2). that controlled the contact drum. To model a traditional haptic interface, during operator finger motion, while the slave is not in contact with any slave environment objects, the contact drum is position controlled to follow the replicated finger position, offset by 0 to 1 degrees. When contact is made with a virtual object, the contact drum is force controlled to provide a force given by EQ. (1).

In the experiment, twelve subjects were each presented with six surface models for both a traditional control algorithm, and six surface models for the proposed DECAFF control system. The six surfaces were defined by both a high and a low level for each of three variables expected to contribute to the perceptual experience of

the operators. The variables included surface stiffness (K), surface damping constant (B), and rate of communication (S) between the haptic control PC and the VR PC. The subjects were presented surfaces of matching K, B, and S in pairs for both the traditional control and DECAFF system. For each pair of surfaces, subjects were asked to report which surface felt more like a “wall” or “rigid body”. Additionally for each surface, the subject reported the location where they thought the surface began, or the finger position at which they made initial contact with the surface.

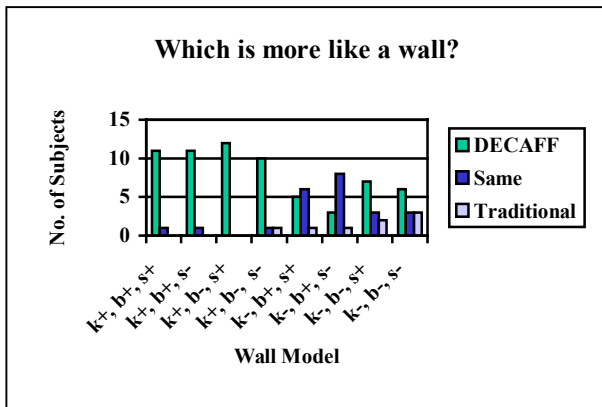


Figure 9 Subjects' Perception of Wall Models

Figure 9 shows the perception of subjects as the number reporting which control method felt more like wall, based on surface model variables. For surfaces with high K and high B levels, subjects overwhelmingly chose the DECAFF system as that which was more like a wall. As the surface models become “softer” or of a low K value, the proportion of subjects reporting DECAFF was more like a wall [was reduced](#) ~~approached 50% or a random chance value.~~

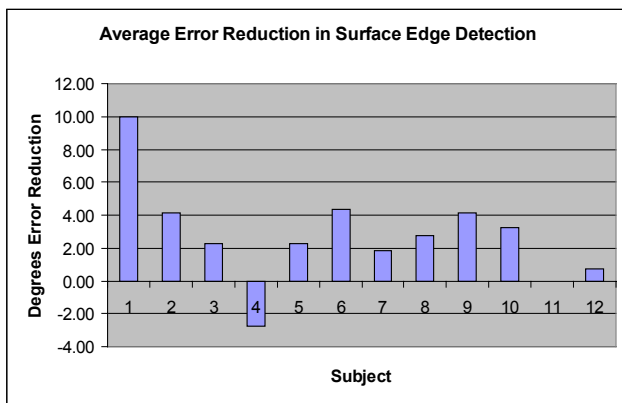


Figure 10 Average Error Reduction in Edge Detection (Degrees)

In order to further quantify the difference in sensitivity of perception of surfaces between traditional control and DECAFF, the error between the actual surface position and the subject's reported perception of the surface position was calculated. The average error reduction across all surface models of the DECAFF system vs. traditional control is shown in FIG. 10. In the figure, positional data

is shown in degrees, which was the variable measured in the experiment.

Some subjects demonstrated an exceptionally higher accuracy than others did in their ability to identify the surface locations for both control methods. These subjects (e.g. 3 and 9) demonstrated the highest accuracy percentage improvement (over 85%) as shown in FIG. 11. On average only two of the twelve subjects did not show an improvement with their accuracy in surface edge locations. Subject 11 was able to equally accurately detect surface locations for both control methods, while subject 4 was able to more accurately detect locations while using the traditional control. The average improvement in surface detection accuracy for the DECAFF system across all subjects and all wall models was 2.75 degrees and 36.8%.

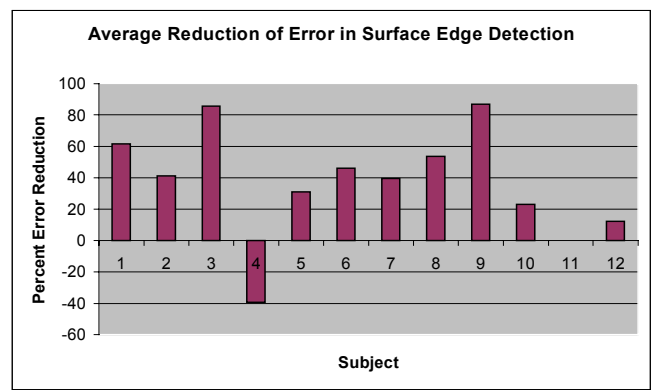


Figure 11 Average Error Reduction in Edge Detection (Percent)

6. Conclusions

In this paper a new design of a multi-fingered haptic interface has been discussed. Several advantages of this new design have been outlined. The new design provides an interface mechanism that is lightweight, comfortable, with a large workspace, and delivers force display substantially normal to the operator's fingertips throughout a full 180 degree range of finger bend motion. Further, the design demonstrates high transparency and introduces a new [DECAFF](#) control algorithm that permits several previously cited deficiencies in haptic interfaces to be addressed. Through the use of a decoupled actuator, the design presented here allows for better haptic rendering of rigid surfaces and more rapid delivery of haptic sensations. This control method offers a significant contact display speed advantage over previously reported haptic interfaces for grasping tasks, which at best only provide a signal to the user in the calculation cycle *following* the one in which the slave finger contacts or penetrates the grasped object. In the present method, contact between the robotic (or virtual) finger and an object can be displayed instantaneously, since the contact drum is in the proper position *prior* to robotic (or virtual) finger and object contact. The present system with a decoupled actuator and the above described position control overcomes the instability problem of interacting with high stiffness virtual objects during grasp tasks. Preliminary human perception study results demonstrate a clear and consistent improvement in both the perceptual quality of rigid surfaces, and the sensitivity (or accuracy) at which subjects can detect the presence of the surface.

7. References

1. Ascension Company web page <http://www.ascension-tech.com/>.
2. Burdea, G., 1996, Force and Touch Feedback for Virtual Reality, John Wiley and Sons, New York, NY.
3. Colgate, J., Grafing, P., Stanley, C., and Schenkel, G., 1993, Implementation of Stiff Virtual Walls in Force Reflecting Interfaces, *Proceedings of Virtual Reality Annual International Symposium*, IEEE Neural Networks Council, Piscataway, NJ, pp. 202-215.
4. Cutkosky, M. and Howe, R., 1990, "Human Grasp Choice and Robotic Grasp Analysis" in S. Venkataraman and T. Iberall Editors, *Dextrous Robotic Hands*, Springer Verlag, New York, pp. 5-31.
5. Kazerooni, H., 1993, Human Induced Instability in Haptic Interfaces, *Proceedings of the 1993 ASME Winter Annual Meeting*, DSC-Vol. 49, pp 15-27.
6. Klatzky, R., Purdy, K., and Lederman, S., 1996, When is Vision Useful During a Familiar Manipulatory Task ?, *Proceedings of the 1996 ASME International Mechanical Engineering Congress and Exposition*, DSC-Vol. 58, ASME, New York, NY, pp. 561-566.
7. Kramer, J., 1993, Force Feedback and Textures Simulating Interface Device, U. S. Patent No. 5,184,319, USPO.
8. Lawrence, D, Salada, M., Lucy, P., and Dougherty, A., 1996, Quantitative Experimental Analysis of Transparency and Stability in Haptic Interfaces, *Proceedings of the 1996 ASME International Mechanical Engineering Congress and Exposition*, DSC-Vol. 58, ASME, New York, NY, pp. 441-449.
9. Schulteis, T., Dupont, P., Millman, P., and Howe, R., 1996, Automatic Identification of Remote Environments, , *Proceedings of the 1996 ASME International Mechanical Engineering Congress and Exposition*, DSC-Vol. 58, ASME, New York, NY, pp. 451-458.
10. Shimoga, K., Murray, A., Khosla, P., 1996, A Touch Display System for Interaction with Remote and Virtual Environments, *Proceedings of the 1996 ASME International Mechanical Engineering Congress and Exposition*, DSC-Vol. 58, ASME, New York, NY, pp. 523-529.
11. Springer, S., Gadh, R., 1996, State-of-the-art Virtual Reality Hardware for Computer-aided-design, *Journal of Intelligent Manufacturing*, Volume 7, pages 457-465, December, 1996.
12. Springer, S., Gadh, R., 1997, Haptic Feedback for Virtual Reality Computer Aided Design, *Presented at the 1997 ASME International Mechanical Engineering Congress and Exposition*, November 1997, Dallas, TX, ASME, New York, NY.
13. Springer, S., Ferrier, N., A New Method for Design and Control of Haptic Interfaces for Display of Rigid Surfaces, *Presented at the 1999 ASME International Mechanical Engineering Congress and Exposition*, November 1999, Nashville, TN, ASME, New York, NY. (to appear)
14. Springer, S., 1999, Design and Control of Multi-finger Haptic Interfaces for Improved Perceptual Experiences in Teleoperational Grasping, doctoral thesis at the University of Wisconsin-Madison, ~~December~~ August 1999, (to appear)
15. Virtual Technologies, Inc., 1997, company web page <http://www.virtex.com>